ISTITUTO NAZIONALE DI FISICA NUCLEARE

Laboratori Nazionali del Gran Sasso

INFN - 23 -29 LNGS
24 ottobre 2023

Structural analysis of the double-walled copper-steel cryogenic chamber of the ASTAROTH experiment

Daniele Cortis[1], Donato Orlandi[1], Andrea Zani[2], Davide D'Angelo[2,3]
[1)]*INFN, Laboratori Nazionali del Gran Sasso, via G. Acitelli 22, 67100, L'Aquila, IT*
[2)]*INFN Sezione di Milano, via Celoria 16, 20133 Milano, IT*
[3)]*Università degli Studi di Milano, Dip. di Fisica, via Celoria 16, 20133 Milano, IT*

Abstract

This document describes the verification process of structural performance of the double-walled copper-steel cryogenic chamber of the ASTAROTH (All Sensitive crysTal ARray with lOw THreshold) experiment and the evaluation of the stresses generated near the thermal bridge connecting the inner and outer wall. The chamber consists of an external AISI 316L stainless steel dewar and an inner double-walled OF (Oxygen Free) copper dewar connected to an AISI 316L stainless steel flanged collar. The results showed that close to the thermal bridge (copper-steel junction) the stresses slightly exceed the YS of copper at the estimated operating temperature (localised strain-hardening condition). On the other hand, the safety coefficient respect to fracture is well above one for both materials. This condition, together with the fact that limited cooling cycles are expected during the operating life of the system, leads to the assumption that a progressive material hardening will occur in this area, thus locally raising the YS limit.

Published by
Laboratori Nazionali di Frascati

Summary

1 Introduction

This document describes the verification process of structural performance of the double-walled copper-steel cryogenic chamber of the ASTAROTH (All Sensitive crysTal ARray with lOw THreshold) experiment [1] and the evaluation of the stresses generated near the thermal bridge connecting the inner and outer wall.

The detector, thanks to an innovative concept for Dark Matter research, employs a silicon photomultiplier array (SiPM) to read the scintillation light produced by thallium-doped sodium crystals, Nal (TI). Since the use of SiPM requires the system to operate under cryogenic conditions (< 100 K), liquid Argon (LAr) was chosen, also due to the possibility of using this element as a secondary veto detector around NaI (TI) crystals. This solution, together with the use of radio-pure materials for the manufacture of the system, is crucial for the suppression of the radioactive background.

The chamber consists of an external AISI 316L stainless steel dewar and an inner double-walled OF (Oxygen Free) copper dewar connected to an AISI 316L stainless steel flanged collar. (Figure 1). The function of the collar is to maintain the two walls at different temperatures through the high thermal resistance generated by the different conduction coefficients of the two materials (~15 vs 400 W/mK at a temperature of 295 K). The system, immersed in a bath of liquid Argon (LAr) at a temperature of 87 K and a pressure of 1 bar (0.1 MPa), contains up to two Nal (TI) scintillators. The double-wall cavity of the stainless steel - copper chimney will be kept under vacuum to limit heat exchange with the LAr bath to radiation (between the two copper walls) and conduction through the thermal bridge. The copper chamber will be filled with Helium (He) gas in under pressure (final goal: 0.01 MPa) to limit conduction. It will be kept at an operating temperature of ~150 K: thermal equilibrium is achieved using a dedicated heater of ~190 W located around the circumference of the inner wall. The volume around the two scintillators is further thermally shielded from the top of the chimney with the help of a copper disks. Further stainless steel disks will be placed stainless steel in the upper part of the chimney to force gas stratification and minimize convection.

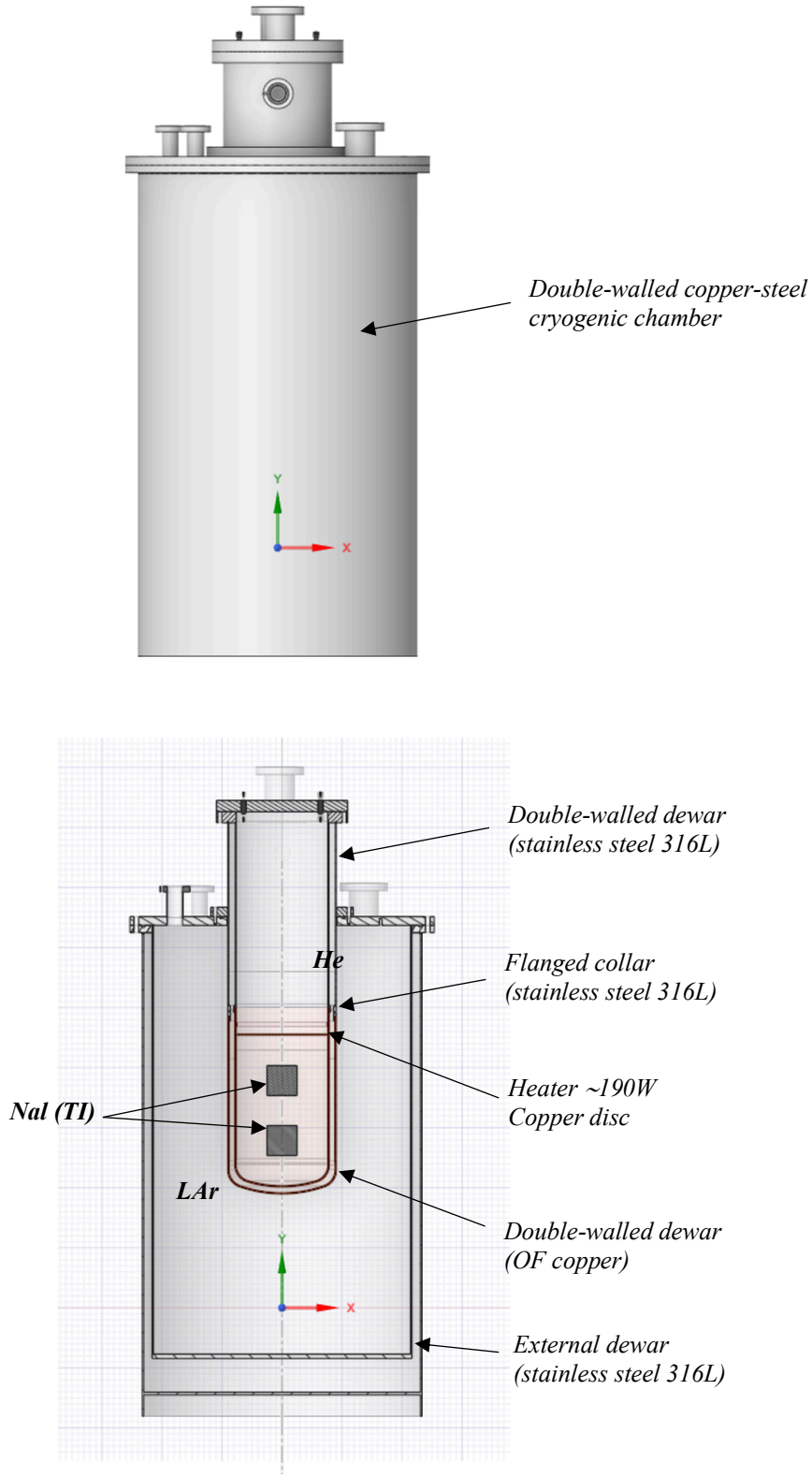

Figure 1: Double-walled copper-steel cryogenic chamber.

2 Materials properties

The material properties (OF copper and AISI 316L stainless steel), up to cryogenic chamber operating conditions (~87 K), were identified by studying the literature [2, 3] and using the available databases [4, 5] within the software used for the analysis: ANSYS® Workbench 2020R2.

The behaviour of the thermal conductivity (C_t), expansion coefficient (C_e) and Young's modulus (E) employed within the simulations to verify the structural performance, are shown below. The behaviour of the materials was modelled using an elastic-linear model without strain hardening [6], because of the cryogenic chamber is not expected to operate in the plastic region, beyond the yield strength of the material.

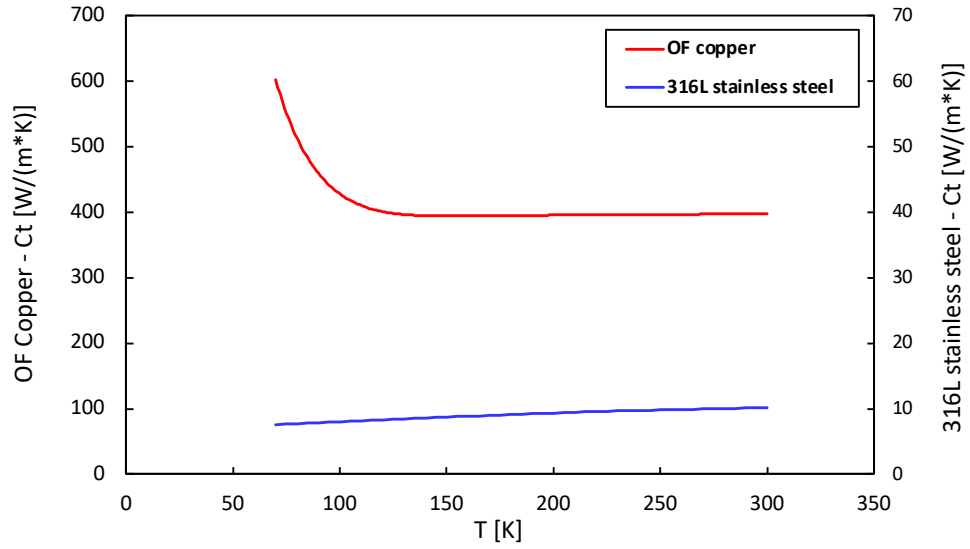

Figure 2: Thermal conductivity (C_t) of OF copper and AISI 316L stainless steel [2,3].

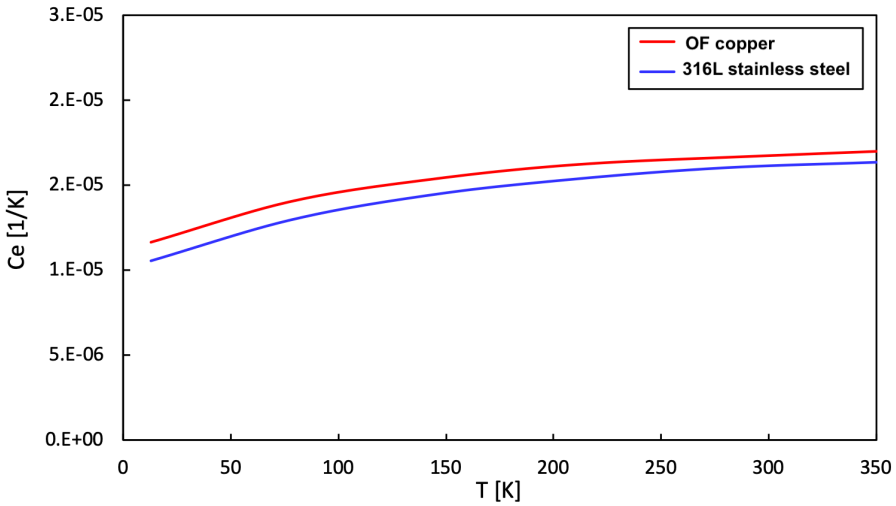

Figure 3: Expansion coefficient (C_e) of OF copper and AISI 316L stainless steel [2, 3].

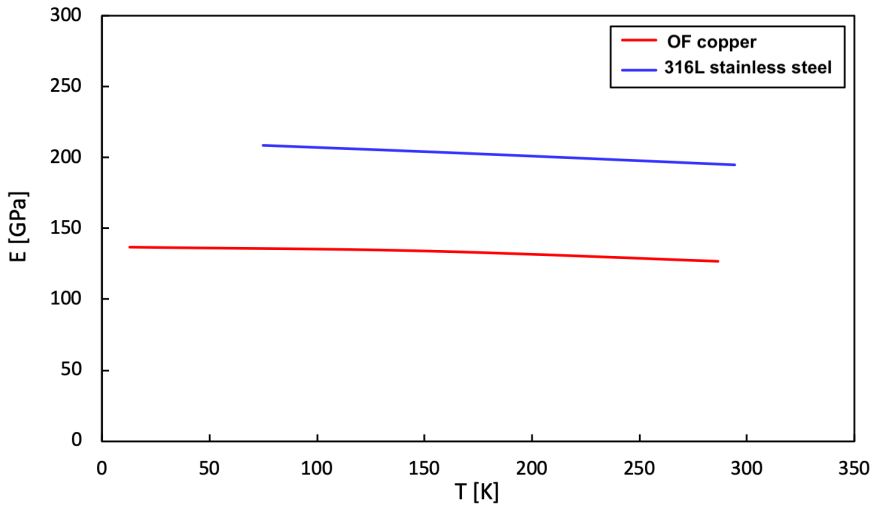

Figure 4: Young's modulus (E) of OF copper and AISI 316L stainless steel [2, 3].

Table 1 and 2 show the Yield Stress (YS) and the Ultimate Tensile Stress (UTS) values, which were used to evaluate the results and whether the yield condition was reached.

Table 1: Mechanical properties of OF copper [4].

T [K]	YS [MPa]	UTS [MPa]
295	46.2	215.8
195	45.5	264.1
76	51.0	348.9
20	57.9	439.9
4	54.5	416.4

Table 2: Mechanical properties of AISI 316L stainless steel [3, 5].

T [K]	YS [MPa]	UTS [MPa]
300	216	530
77	314	1235
4	431	1440

The annealing material physical state of materials has been chosen to describe of mechanical properties, since it is closer to the condition of the cryogenic chamber after the vacuum brazing process of the copper-steel double-wall (i.e., localised heating near the thermal bridge).

3 Preliminary thermal analysis: comparison between CFD and FEM modelling

Typically, a thermo-structural analysis can be performed coupling different physical models and mathematical equations, with the aim of discretizing the thermal and/or deformation field of a component subjected to different boundary conditions.

In this scenario, to evaluate if the resulting thermal field in the He volume was better described by a fluid model (CFD - Computer Fluid Dynamics) or a solid model (FEM - Finite Element Method), a preliminary two-dimensional (2D) simulation has been performed. The first one, using the Navier-Stokes equations (conservation of mass, momentum, and energy), can simulate the behaviour of a gas by considering the contribution of conduction, convection, and radiation, as well as the possibility of describing the presence of turbulent motions within the fluid. The second, based on the finite element method, is instead able to describe the heat exchange within a gaseous volume solely by conduction, neglecting the other contributions.

The boundary and operating conditions of the cryogenic chamber, where the heat exchange between fluids occur slowly and mainly by conduction, suggest that there should be no substantial difference between the two models, and that the conductive contribution has the greatest effect in the definition of the thermal field inside the He volume. However, the presence of a high thermal gradient between the copper-steel double-wall suggests a locally more complex gas behaviour, which can be better described by a fluid model. For this reason, before carrying out a thermo-structural analysis considering all the design elements of the chamber, it was decided to compare the two methodological approaches to choose the most suitable one for this application.

Figure 5 shows the simplified two-dimensional (2D) model of the cryogenic chamber used for both the CFD and FEM analyses. In both cases, the same boundary conditions were applied (Table 3). The software used for the analyses is ANSYS Workbench 2022R2: the “Fluent” environment for the CFD model and the “Mechanical” one for the FEM model.

Table 3: CFD e FEM Model, boundary conditions.

Boundary conditions	CFD	FEM
Upper flange temp.	288 K	
Bottom flange temp.	268 K	
External dewar temp.	87 K	
Heater power	2.8E-02 W/mm^3	

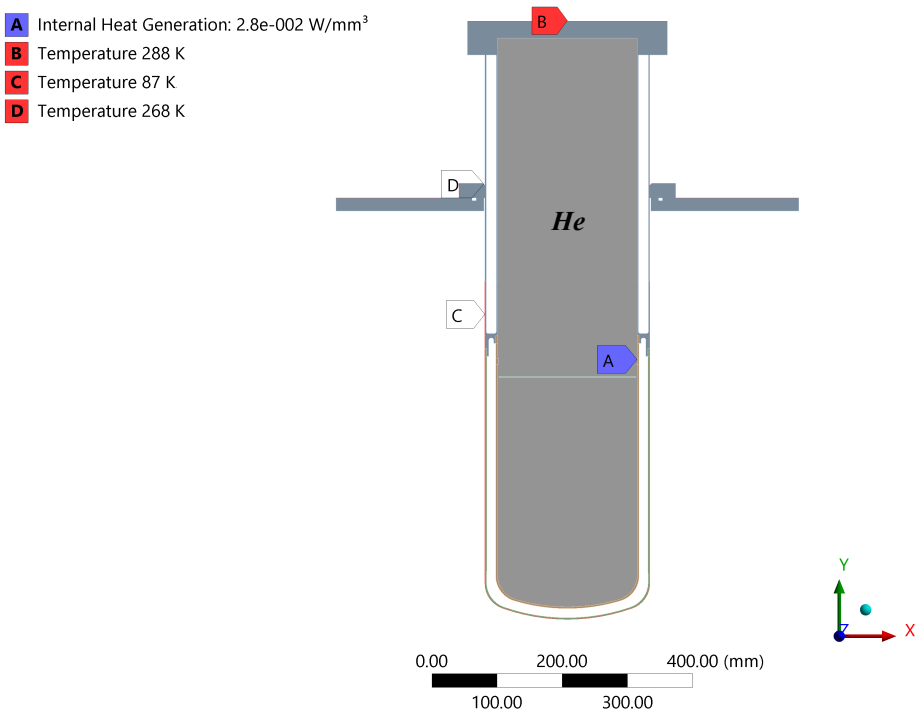

Figure 5: Two-dimensional (2D) model of the cryogenic chamber.

The simplified two-dimensional (2D) model considers the two flanges, the double-walled copper-steel dewar and the theoretical temperatures on the different walls: 288 K for the upper flange, 268 K for the lower flange and 87 K for the outer wall of the dewar in contact with the LAr. The presence of the heater on the inner copper wall of the dewar (~190 W, equal to ~2.8E-02 W/mm^3) was also considered. The resulting thermal field within the He volume is shown in Figure 6.

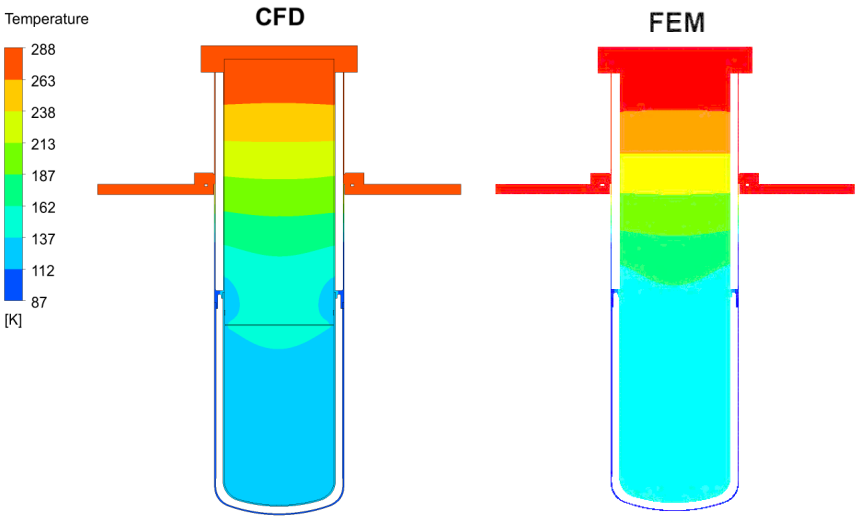

Figure 6: CFD and FEM model, resulting thermal field within the He volume.

The comparison between the thermal fields shows, as expected, that there are no substantial differences between the methodologies as long as the thermal gradient is limited to 100 K and it is far enough from the thermal bridge. The CFD model, despite some simplifications adopted (e.g., laminar motion of the fluid) can describe the gradient in this area more accurately; the thermal gradient is also influenced by the presence of the copper disc above the two scintillators.

To better assess the quantitative differences between the two models, the temperature (T) within the He volume along the axial symmetry axis of the cryogenic chamber is shown in Figure 7. The plots shows that the greatest difference is located closely to the thermal bridge. Despite this, the maximum temperature difference (~16 K) remains acceptable and it is sign of the rightness of the results obtained with two different approaches. Also, for the FEM analysis, the temperature of 151 K agrees with the design goal of 150 K.

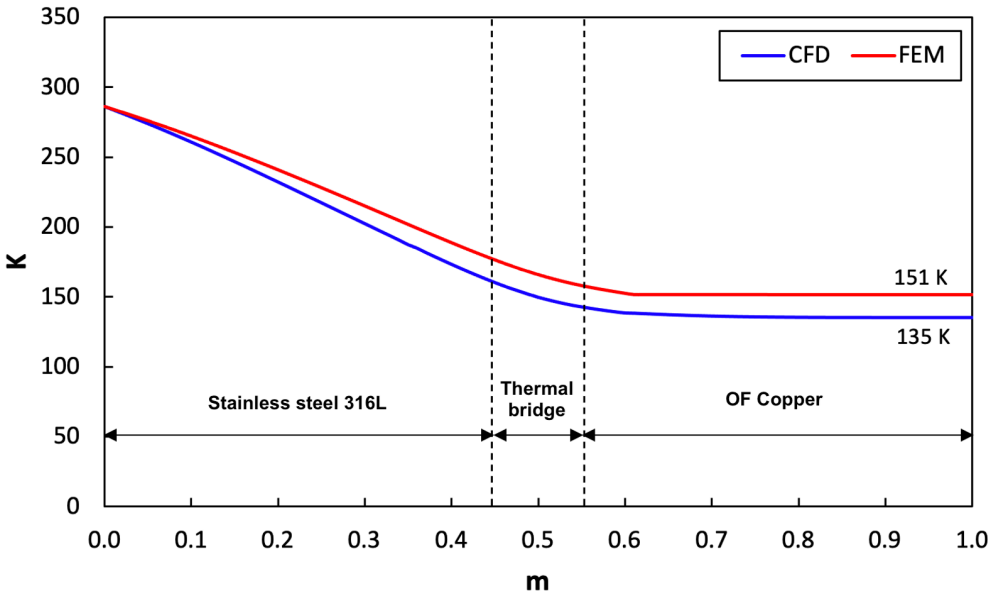

Figure 7: CFD and FEM model, temperature along the axial symmetry axis of the cryogenic chamber.

The results show that, under these boundary conditions, a fluid model, even when used in a simplified form, can better describe the behaviour of a gas volume than a solid model.

In the next paragraph, to simplify the structural analysis (e.g., automatic mapping of the thermal field) and to have a more conservative approach (a higher thermal gradient produces higher stress in the material), it was decided to apply the FEM model, being confident that any overestimation of the temperature within the He volume can be tuned by the internal heater.

4 Thermo-structural analysis: multi-physics coupled simulation

The thermo-structural analysis of the cryogenic chamber was carried out using the ANSYS® Workbench 2020R2 software ("Mechanical" environment) discretizing the He volume as a solid body in which the heat is transmitted only by conduction. The obtained thermal field was used as an input boundary condition for the stress analysis of the chamber near the copper-steel junction.

The three-dimensional (3D) model of the chamber was simplified by removing the details not useful for analysis. The circumferential symmetry of the system (45°) was also used to simulate only 1/8 of the complete model (Figure 8). This simplification made possible to reduce the computational time and to use a finer mesh in the most stressed area of the thermal bridge (copper-steel junction).

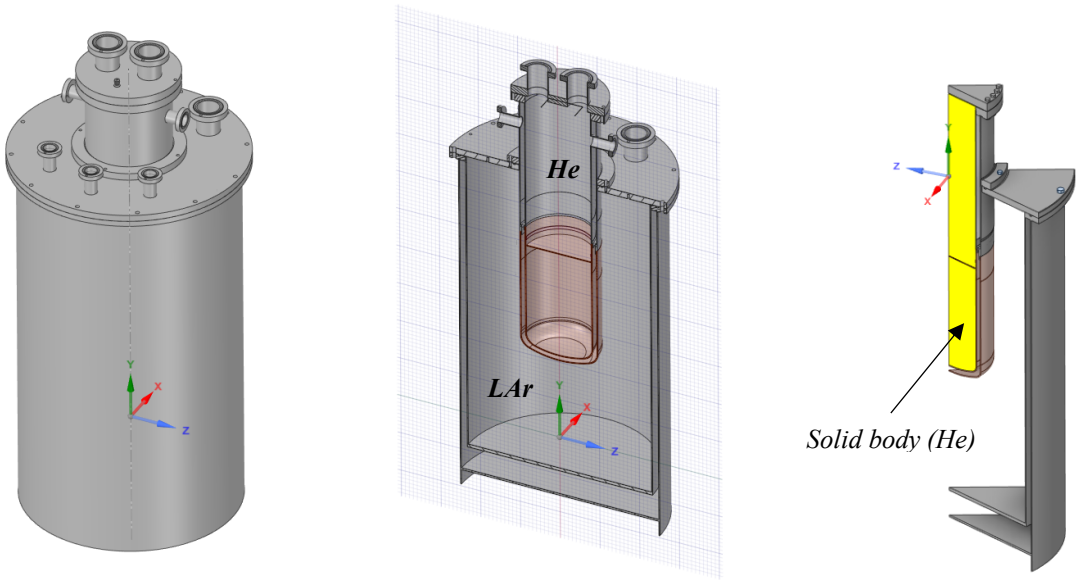

Figure 8: The three-dimensional (3D) model of the chamber.

Firstly, a sensitivity analysis of the mesh was carried out to identify the optimal elements size (quadratic order) near the copper-steel junction (Table 4).

Table 4: Sensitivity mesh analysis.

N.	External dewar mesh size [mm]	Internal dewar mesh size [mm]	Copper-steel junction mesh size [mm]	Von Mises stress [MPa]
1°	5.0	3.0	2.0	56.8
2°			1.5	54.5
3°			1.4	50.9
4°			1.3	50.4

The thermal analysis was then performed on the simplified model applying the same boundary conditions described in the previous paragraph (Table 3). The resulting thermal field is shown in Figure 9: the temperature distribution confirms the outcomes of the preliminary thermal analysis (Figure 6).

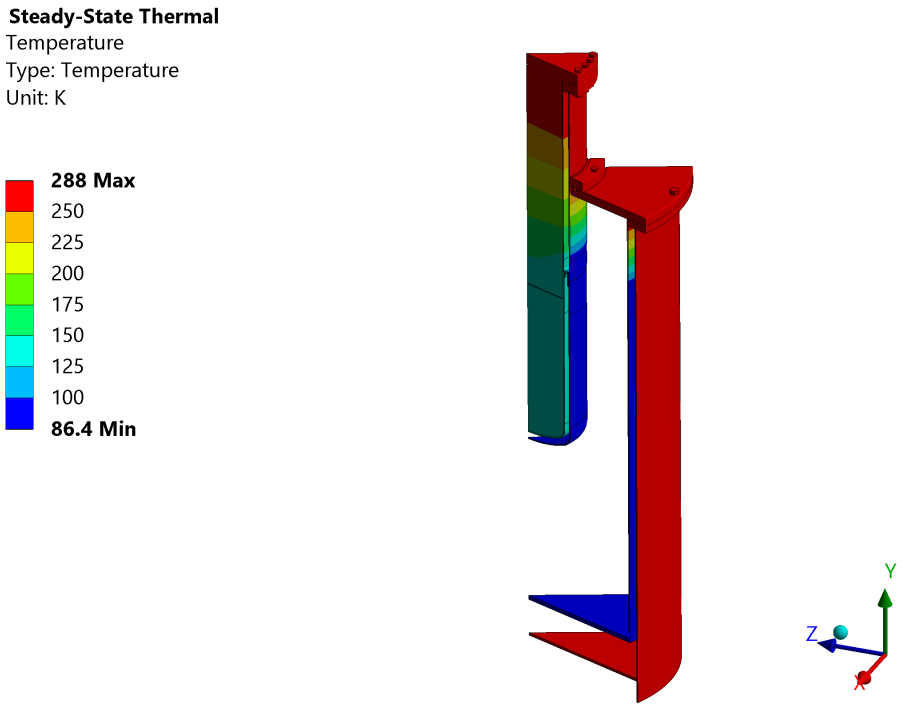

Figure 9: Resulting thermal field of thermal analysis.

The resulting thermal field was then used as the input boundary condition for the structural analysis; also, the following boundary conditions were applied to the cryogenic chamber model (Figure 10):

- the pressure on the outer wall of the dewar in contact with the LAr (0.1 MPa) and pressure on the inner wall (0.01 MPa) where there is the He gas
- the pre-load of the bolts (1/4 of the rupture load)
- the static friction coefficient between the steel flanges (0.8)
- the acceleration of gravity (9.81 m/s)
- the contact of the external dewar with the ground

The structural analysis, consisting of 570,000 elements and 1,200,000 nodes, was carried out with a dedicated workstation (CPU: Intel Xeon Gold 6246R CPU @ 3.40GHz, RAM: 256 GB, GPU: NVIDIA Quadro RTX 5000) and took ~ 2 hours and 20 min to calculate the solution.

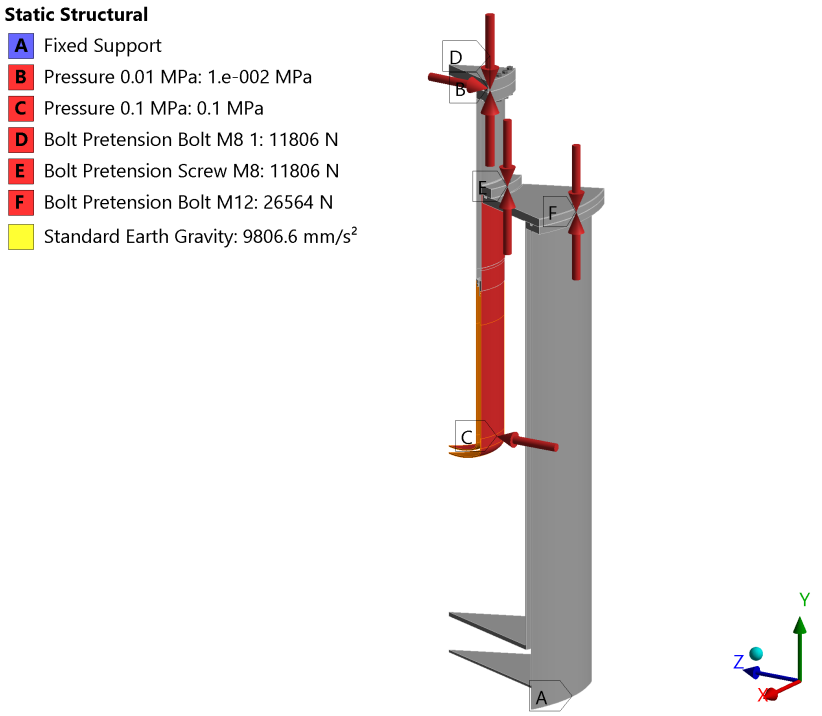

Figure 10: Boundary condition of the structural analysis.

The results of the structural analysis are shown in Figures 11 and 12. The first one shows the deformation field of the entire chamber, highlighting how the maximum deformation is located at the bottom of the external dewar (~2.2 mm), unlike the copper chamber (1.2 mm); the second one shows the stresses generated near the thermal bridge (max 169.4 MPa on the steel wall).

Regarding to the steel wall, the maximum stress is below the YS limit at the operating temperature of 87 K, while for the copper wall, estimated to be at an operating temperature of 140 K, the maximum stress is 50.4 MPa, slightly above the YS limit (48 MPa, linearly interpolating the values of Table 1). In this context, the copper is in a condition of localised strain-hardening, presenting a safety coefficient less than one (Table 5). A more focused analysis of the stress distribution in this area (Figure 13) shows that the highest values are between 45 and 50 MPa, localised along a circular band of 4 mm, without affecting the overall section of the copper wall. On the other hand, the safety coefficient respect to fracture is well above one for both materials (Table 5).

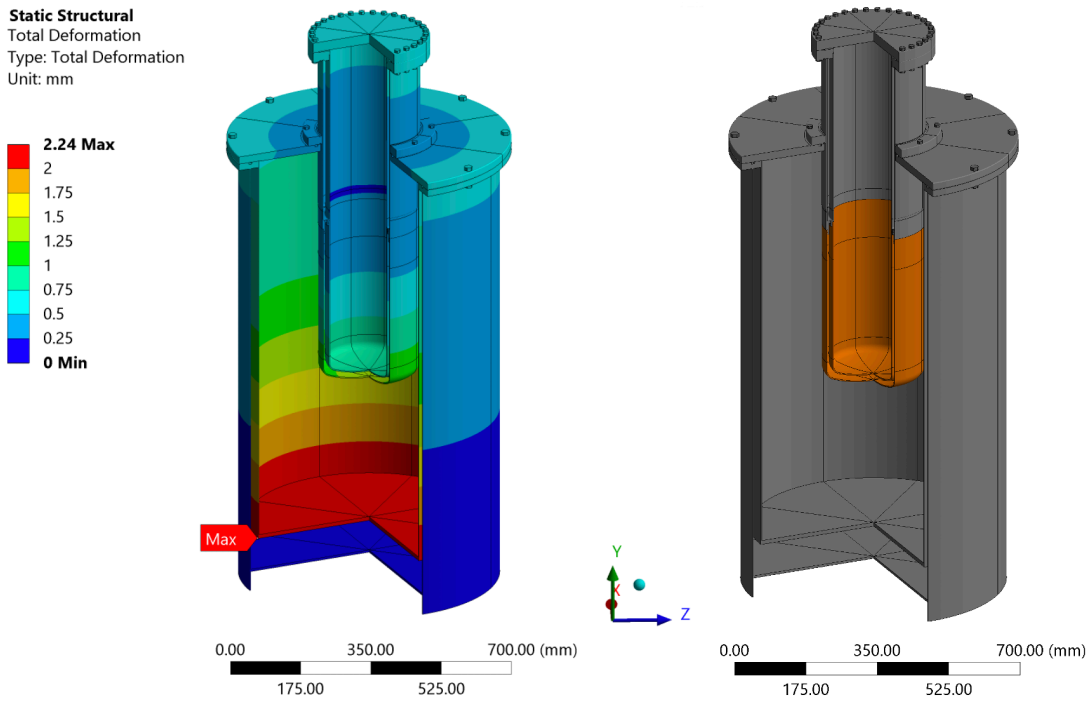

Figure 11: Deformation field of the entire chamber.

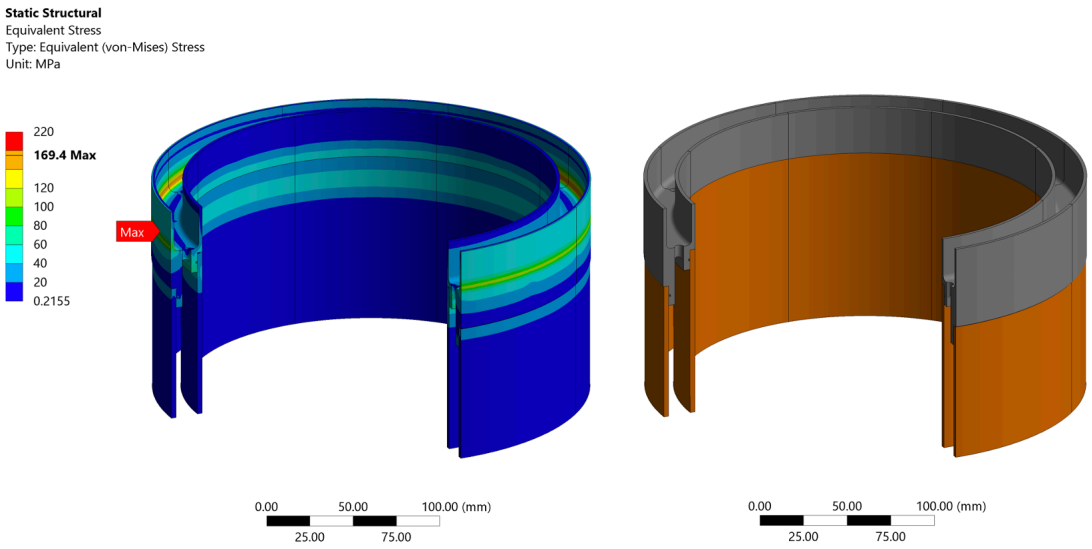

Figure 12: Stresses distribution near the thermal bridge of the chamber.

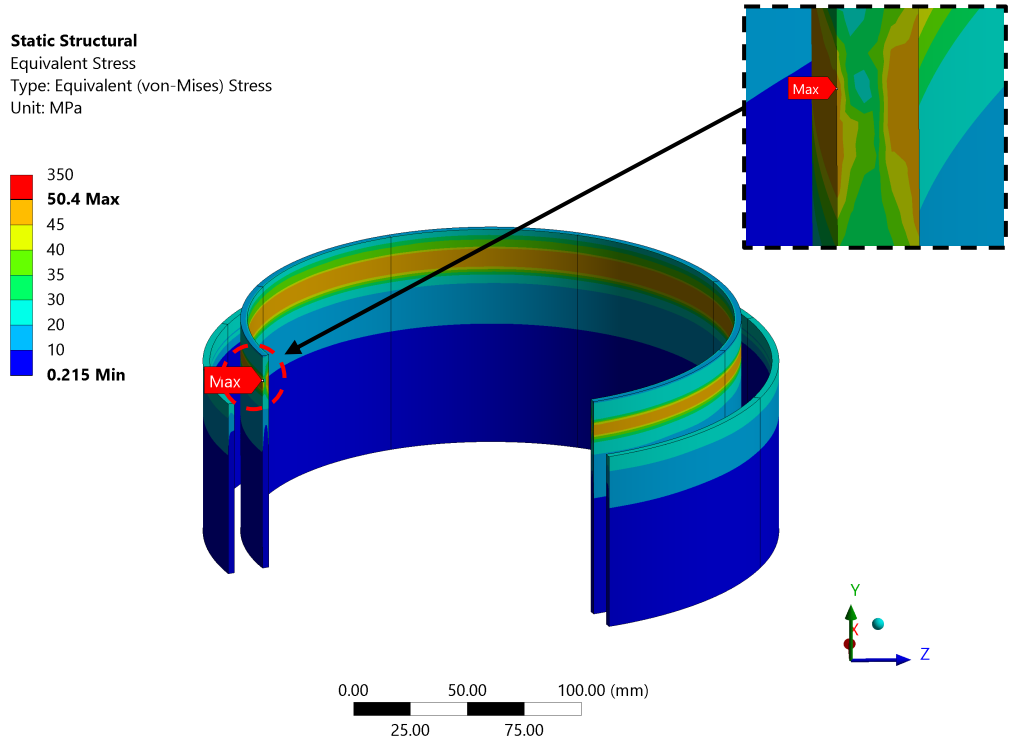

Figure 13: Stresses distribution near the thermal bridge of the chamber (copper wall).

Table 5: Safety coefficients respect to YS and UTS.

Material	YS [MPa]	UTS [MPa]	Von Mises stress [MPa]	Safety coefficient respect to YS	Safety coefficient respect to UTS
316 L	314 @ 77 K	1235 @ 77 K	169.4	1.86	7.29
Cu OF	48 @ 140 K*	300 @ 140 K*	50.4	0.96	5.95

* *estimated linearly interpolating the values of Table 1*

This condition, together with the fact that limited cooling cycles (3/4 per year) are expected during the operating life of the system, leads to the assumption that a progressive material hardening will occur in this area, thus locally raising the YS limit. Therefore, it is advisable to initially reach an operating temperature of 87 K with progressive cooling/heating cycles, to gradually hardened the copper wall near the thermal bridge increasing the YS limit, and making the system operate in the elastic field condition.

5 Conclusions

This document describes the verification process of structural performance of the double-walled copper-steel cryogenic chamber of the ASTAROTH (All Sensitive crysTal ARray with lOw THreshold) experiment and the evaluation of the stresses generated near the thermal bridge connecting the inner and outer wall.

The chamber consists of an external AISI 316L stainless steel dewar and an inner double-walled OF (Oxygen Free) copper dewar connected to an AISI 316L stainless steel flanged collar. The results show that, under these boundary conditions, a fluid model, even when used in a simplified form, can better describe the behaviour of a gas volume than a solid model.

Despite that, to simplify the structural analysis (e.g., automatic mapping of the thermal field) and to have a more conservative approach (a higher thermal gradient produces higher stress in the material), it was decided to apply the FEM model, being confident that any overestimation of the temperature within the He volume can be tuned by the internal heater.

The results showed that close to the thermal bridge (copper-steel junction) the stresses slightly exceed the YS of copper at the estimated operating temperature (localised strain-hardening condition). On the other hand, the safety coefficient respect to fracture is well above one for both materials. This condition, together with the fact that limited cooling cycles are expected during the operating life of the system, leads to the assumption that a progressive material hardening will occur in this area, thus locally raising the YS limit.

More analyses on the experimental behaviour of the copper material used for the manufacture of the cryogenic chamber, under operating conditions (e.g., vacuum welding process and localised annealing near the thermal bridge), were conducted at the "Accelerators and Applied Superconductivity Laboratory" (LASA) in Milan. Tensile and bending tests were performed with standardised copper samples produced by the company from the same material used for the chamber.

References

[1] A. Zani et al., The ASTAROTH Project: enhanced low-energy sensitivity to Dark Matter annual modulation, Journal of Physics: Conference Series, Volume 2156, 17th International Conference on Topics in Astroparticle and Underground Physics (TAUP 2021), 26 August-3 September 2021, Valencia. http://dx.doi.org/10.1088/1742-6596/2156/1/012060

[2] Copper, C10200, soft (oxygen-free h.c. copper). Data compiled by the Granta Design team at ANSYS, incorporating various sources including JAHM and MagWeb.

[3] Stainless-steel 316L (Low Carbon). Data compiled by the Granta Design team at ANSYS, incorporating various sources including JAHM and MagWeb.

[4] Copper Development Association Inc. Mechanical Properties of Copper and Copper Alloys at Low Temperatures. Copper 122: Phosphorus Deoxidized, High Residual Phosphorus (Annealed).

[5] R.L. Tobler, A. Nishimura and J. Yamamoto, Design-Relevant Mechanical Properties of 316-Type Stainless Steel for Superconducting Magnets, National Institute for Fusion Science, 1996.

[6] J. Shigley, R. Budynas, J. Keith, Mechanical Engineering Design, McGraw-Hill, 2014.